LiDAR-based estimation of forest floor fuel loads using a novel distributional approach

Jan A.N. van Aardt[1], Mary Arthur[2], Gretchen Sovkoplas[2] & Tyson Lee Swetnam[3]

[1]Rochester Institute of Technology, Rochester, NY, USA; vanaardt@cis.rit.edu
[2]University of Kentucky, Lexington, KY, USA; marthur@email.uky.edu & gretchen.sovkoplas@uky.edu
[3]University of Arizona, Tucson, AZ, USA; tswetnam@arizona.edu

Abstract. Light detection and ranging (LiDAR) has seen significant application across a range of forest structural assessment applications, ranging from forest volume and biomass assessment, to ecological applications such as leaf area and fuel load modelling. However, quantification of sub-canopy structure remains a challenge, especially when considering downed coarse woody debris (CWD) near the ground surface. This is true because the LiDAR signal attenuates through the canopy, LiDAR systems can be set to record the last of many returns, which is often the ground itself, and there is a system-specific vertical resolution that influences detection of structure in-between returns. We applied a LiDAR distributional approach to CWD modeling that included both above-ground and theoretical "below-ground" returns, with the latter being attributed to multiple scattering effects. This was done for oak dominant forests in central Appalachia, Kentucky, USA. Medium-fast (10h) and medium-slow (100h) CWD fuel loads exhibited the best results; e.g., an adjusted $R^2 = 0.99$ and a root mean square error value of 0.111 Mg/ha (4.7% of the mean) were achieved for 100h CWD fuel loads. Independent variables included a balanced set from both the above- and below-ground distributions. Results hint at the significant potential of extending distributional approaches to CWD estimation.

Keywords: LiDAR, Coarse woody debris, fuel load, distributional analysis.

1. Introduction

The assessment of forest structure, e.g., volume, biomass, leaf area index (LAI), etc., remains a priority for forest managers and ecologists for reasons ranging from taking stock inventory, performing carbon assessment, and investment planning, to tracking invasive dynamics. One important motive for structural assessment, however, revolves around the need to better understand fire dynamics as a function of fuel load, among other things. For example: Forest managers increasingly are applying prescribed fire as a management tool in the central and southern Appalachian hardwood regions of the United States (Brose *et al.*, 2001). This use of fire as a tool, instead of a reactive management response, is based on a better understanding of the historic (McEwan *et al.*, 2007) roles of fire in this region. In fact, many management plans of national forests throughout the region already include fire as part of their toolkit, e.g., the USDA Forest Service at Daniel Boone National Forest, Kentucky. This increased use of prescribed fires necessitates the need for improved predictions of future burn behavior and improved assessment of the impacts on forest structure, especially at the landscape scale. This is only one of the reasons that light detection and ranging (LiDAR) extensively has been used to characterize forest structural attributes. Not only does such a remote sensing approach enable a synoptic assessment, but LiDAR has emerged as an accurate and precise tool for this purpose.

LiDAR-based assessment of vegetation structure has focused primarily on the assessment of forest volume and biomass and has met with reasonable success (R^2 values typically > 0.80), with studies dating back to the mid-1980s (e.g., Nelson *et al.*, 1988). More recent LiDAR studies have mostly dealt with forest volume and biomass assessment at the plot- and

stand-level (e.g., Lefsky *et al.*, 1999; Næsset, 2002; Popescu *et al.*, 2004; van Aardt *et al.*, 2006). Differentiation also is made between individual tree vs. per-unit-area height distributional approaches (Means *et al.*, 2000; van Aardt *et al.*, 2006). Distinct challenges to such approaches include the scalability of results due to huge data volumes, resource costs, as well as limited extension of work to sub-canopy structure and fuel load applications. Examples of the latter two topics include leaf area index estimation (e.g., Zheng and Moskal, 2009) and fire effects on forest structure (e.g., Hall *et al.*, 2005). However, comprehensive fuel load studies, or detailed sub-canopy structural assessments, remain scarce.

Riaño *et al.* (2003) demonstrated that LiDAR can be used to extract forest fuel distributions from LiDAR data in forests dominated by coniferous and deciduous tree species, but Skowronski *et al.* (2007) highlighted the breakdown of LiDAR-based fuel load assessment for larger areas. Mutlu *et al.* (2008) attempted to improve on LiDAR-only approaches by showing that fuel models can be calibrated using a remote sensing fusion approach that hedges on LiDAR and Quickbird imagery. Beneath the canopy, Seielstad and Queen (2003) have also used small footprint LiDAR data to measure fuel loads of coarse woody debris on the forest floor. This was done by performing "obstacle density" assessment within 2m of the forest floor. We want to expand on such methods by applying a LiDAR distributional approach, similar to those used by Means *et al.* (2000), van Aardt *et al.* (2006), and Pesonen *et al.* (2008). The first two studies focused on forest volume/biomass estimation, while Pesonen *et al.* 2008) highlighted the potential of a distributional approach for coarse woody debris assessment. We propose to improve forest floor fuel load assessment by expanding such distributional approaches to include negative digital elevation model (DEM) residual distributions.

We hypothesize that (i) above-ground LiDAR height distributions are indicative of the downed coarse woody debris (CWD) structure, either through correlations with canopy level structure or via scattering of laser pulses close to the ground and (ii) that so-called negative height residuals, or LiDAR heights that are apparently negative after subtraction of the DEM, potentially contain signal that can be associated with multiple scattering effects. Our objectives therefore are to (i) determine if hypothesized multiple scattering effects and their inclusion in LiDAR distributional analysis can contribute to modeling CWD fuel loads at 1h, 10h, 100h, and 1000h fuel weights and (ii) to assess the relative impact of an increase in DEM spatial resolution, i.e., an increase in "below-ground" returns on the first objective's outcomes. We believe that the multiple scattering effect, caused by a delayed return signal due to vegetation structural complexity (Wu *et al.*, 2009), can be linked to variation in forest floor CWD (Figure 1).

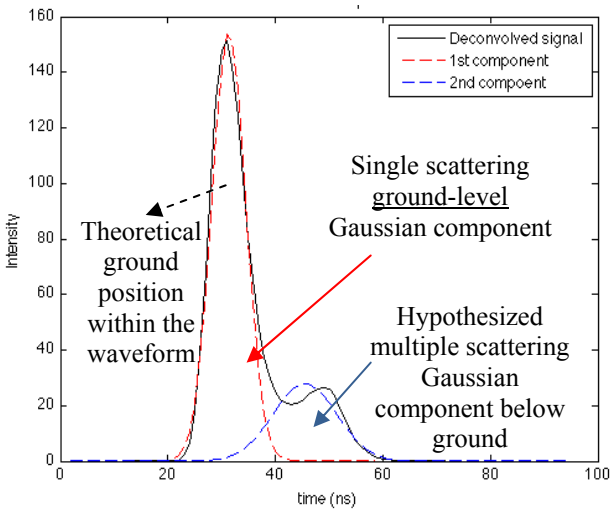

Figure 1: An example of hypothesized multiple scattering effects, i.e., a delayed LiDAR signal that exhibits as being below-ground. This example is from a savanna environment, using an Optech small-footprint waveform LiDAR (0.56 mrad beam divergence). This multiple scattering (blue Gaussian) was attributed to scattering due to dense herbaceous biomass (Wu *et al.*, 2009).

2. Methods

2.1 Study area

The study area is located in the Cumberland district, Daniel Boone National Forest, Kentucky, USA (Figure 2). This central Appalachian region is characterized by upland oak-dominated forests, e.g., scarlet oak (*Quercus coccinea Muench.*) and chestnut oak (*Q. prinus L.*), with some black oak (*Q. velutina Lam.*) and white oak (*Q. alba L.*), where fire-sensitive red maple (*Acer rubrum L.*) and eastern white pine (*Pinus strobus* L.) are gaining dominance.

2.2 Plot establishment

A total of ninety-three plots (10 x 40 m; Figure 3), part of two of the longest running prescribed fire studies on the Cumberland Plateau (Blankenship and Arthur, 2006), have been control-burned at various frequencies. These include a control set, 2003/2009 (infrequent), and 2003/2004/2006/2008 (frequent) burn plots. Plots run 10m uphill and 40m perpendicular to the slope and include January-March, 2009 pre-burn measurements for overstory (trees >10cm diameter-at- breast-height; DBH), midstory includes trees (<10cm DBH in first quadrant), and CWD in terms of 1h, 10h, 100h, 1000h fuels at the fuel transects (pre-burn). The CWD values correspond to 0-0.635cm diameter (1h), 0.635-2.54cm diameter (10h), 2.54-7.62cm diameter (100h), and 7.62 cm diameter (1000h) (Brown *et al.*, 1982). However, our analysis was constrained to 17 pre-burn, frequent burn treatment plots due to LiDAR coverage.

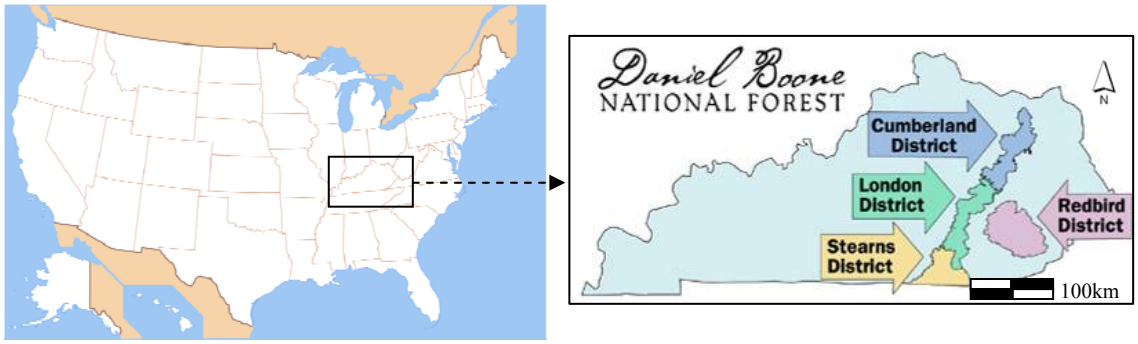

Figure 2: The study area is located in the Cumberland District of the Daniel Boone National Forest.

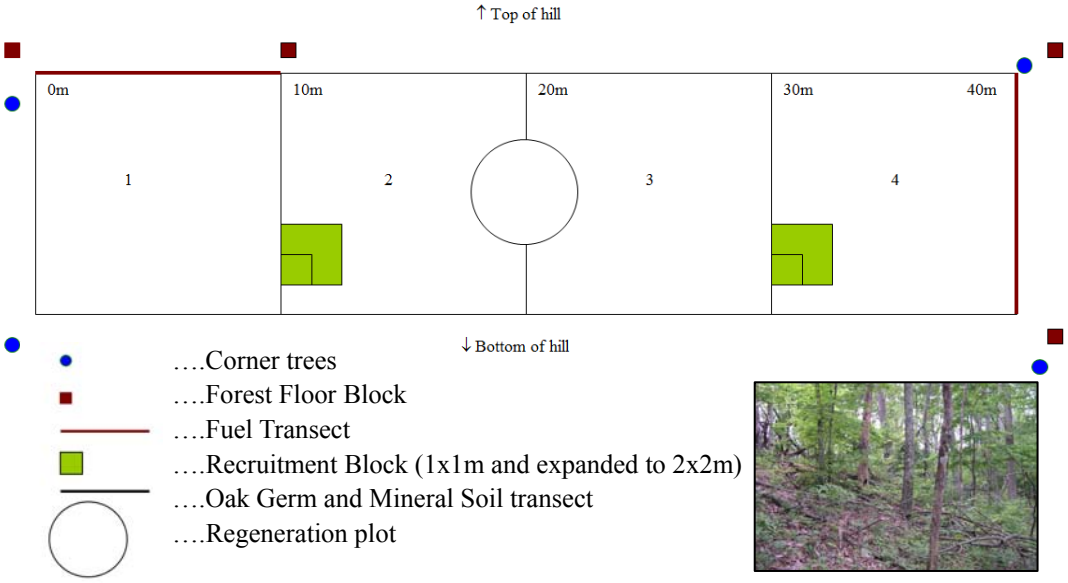

Figure 3: Plot layout for assessment of various forest structural parameters, including a line transect for measurement of CWD. The inset shows an example of a 100h fuel load CWD plot.

2.2 LiDAR data description and analysis

A Leica ALS50 (64KHz pulse rate; 43Hz scan rate; 4 returns/pulse; >5 hits/m^2; 1.4m footprint; 1,655m swath) was used to collect data for the study area during February 2009, prior to the burn treatment. LiDAR returns were classified into ground vs. non-ground returns by the vendor using the well-known Terrasolid slope-radius algorithm (van Aardt *et al.*, 2006). The LiDAR returns subsequently were processed using the following workflow:

1. *DEM generation*: Kriging and nearest neighbor interpolations (Surfer V. 9.0) were used to generate 1m and 10m DEMs of the area. Two interpolation algorithms and spatial resolutions were used to assess the impacts of a theoretically smoother vs. rougher DEM and to determine if resolution impacts derivation of height residuals, respectively. Stated differently, both the interpolation approach and the varying spatial resolutions allowed us to partition the above- and below-ground LiDAR distributions differently.
2. *Residual calculation*: Residuals (height above DEMs) were calculated using Surfer (V. 9.0) in the case of each interpolation algorithm and spatial resolution for the LiDAR point cloud for 25m radius plots, centered on the field plots. We maintained negative residuals, or theoretical below-ground LiDAR returns, which was hypothesized to be related to multiple scattering effects due to scattering by CWD. This is different from most previous approaches, e.g., van Aardt *et al.* (2006), where such returns are set to zero or discarded, since they are assumed to be due to either misclassified ground returns that negatively impact DEM derivation or sensor error.
3. *Modeling*: We generated LiDAR height distribution statistics (see Means *et al.*, 2000; van Aardt *et al.*, 2006) for positive and negative residuals and their associated LiDAR intensities separately. Both sets of distribution statistics were used as inputs to stepwise linear regression (PROC STEPDISC in SAS V. 9.2), with $\alpha = 0.10$ for variable entry to result in <= 10 variables for all CWD models; most models contained < 4 independent variables. CWD models were assessed based on their adjusted R^2 and root mean square error (RMSE) values. These two metrics were considered robust, since they penalize models for overfitting and provide a precision estimate, respectively.

3. Results

Figure 4 shows an example of the below-ground LiDAR return distribution for all the plots based on Kriging at a 10m spatial resolution. While one could argue that such a seemingly normal distribution could be indicative of random system error, it remains striking that the distribution mimics a bell shape for limited multiple scattering close to the ground surface, i.e., fine matter, and a spread-out distribution tail that are theoretically due to fewer, but coarser woody debris objects. Table 1 shows the results of the analysis workflow described above. Results are given in terms of DEM spatial resolution, interpolation method, CWD level, the two model metrics, and the independent variables that were selected as significant to each model.

Table 1: CWD modeling results for all spatial resolutions, interpolation approaches, and CWD fuel levels

Cell	Grid	Fuel	Adj. R^2	*RMSE (Mg/ha)	**Variables
1m	Kriging	1h	0.22	0.102	Canopy02P
		10h	0.38	0.606	StdMeanRefN; StdMeanVegP
		100h	0.41	1.117	P_VegP_10
		1000h	0	N/A	None
	Nearest Neigbor	1h	0.51	0.081	MinVegN; P_VegN_90
		10h	0.46	0.566	P_VegN_90

Cell	Grid	Fuel	Adj. R^2	*RMSE (Mg/ha)	**Variables
		100h	0.74	0.734	P_VegP_90; CVVegN; StdRefN; Canopy01P
		1000h	0	N/A	None
10m	Kriging	1h	0.75	0.058 (16.7%)	StdMeanVegP; MaxVegN; Canopy02P
		10h	0.98	0.11 (9.6%)	MaxVegP; MinVegP; StdMeanVegP; P_VegP_10; MaxVegN; P_VegN_90; MaxRefN; RangeRefN; Canopy02P; Canopy08P
		100h	0.99	0.111 (4.7%)	MeanVegP; CVVegP; SkewnessVegP; StdVegP; MedianVegP; P_VegP_70; CVRefP; P_VegN_75; KurtosisRefN; SkewnessRefN
		1000h	0.69	4.59 (47%)	MinVegP; P_VegP_40; P_VegP_90; Canopy10P
	Nearest Neigbor	1h	0.58	0.075	RangeVegN; Canopy04P
		10h	0.28	0.653	StdMeanRefN
		100h	0.31	1.21	RangeRefN
		1000h	0	N/A	None

*% indicate RMSE as percentage of average fuel weight
****Veg*** = vegetation height return; ***Ref*** = intensity; ***P*** = positive & ***N*** = negative residual

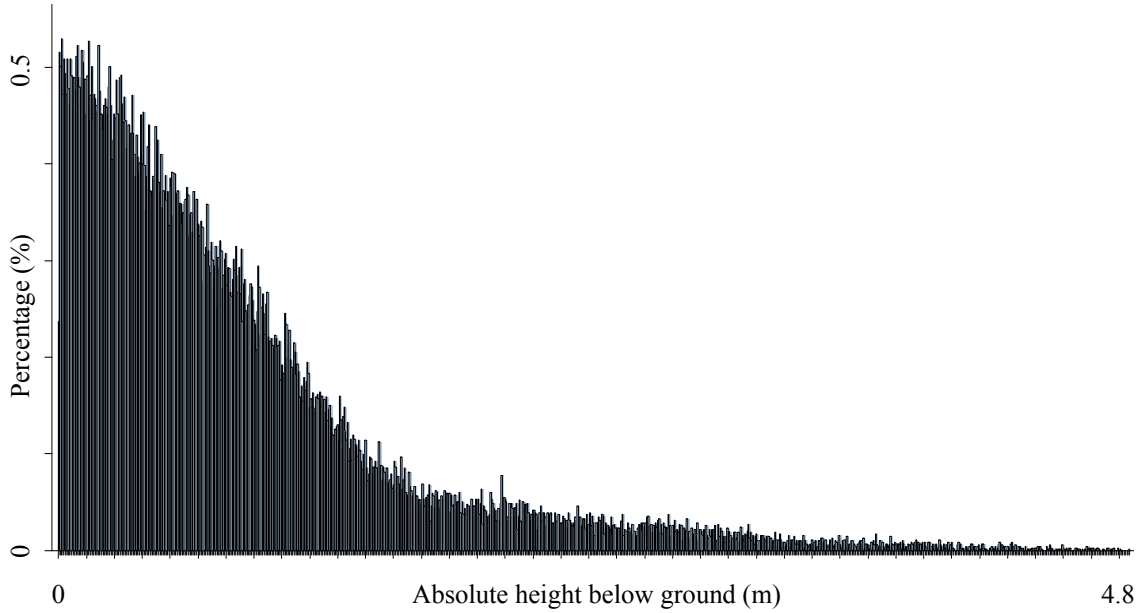

Figure 4: Below-ground return distribution for all plots (Kriging at 10m spatial resolution).

Figures 5 and 6 show the observed vs. predicted model plots for Kriging at 10m spatial resolution and 1h and 10h fuels, respectively. Finally, Figure 7 shows an example of the LiDAR return distribution for the plot that exhibited the smallest RMSE (-0.0001 Mg/ha) for Kriging at 10m and a 100h CWD fuel load. This CWD model included both positive (above-ground) and negative (below-ground) height and intensity residuals. For instance, it is interesting to note that the 75th negative percentile is included as an independent variable - this speaks to the delayed returns, due to hypothesized multiple scattering, that the "coarse" nature of 100h CWD structures would cause.

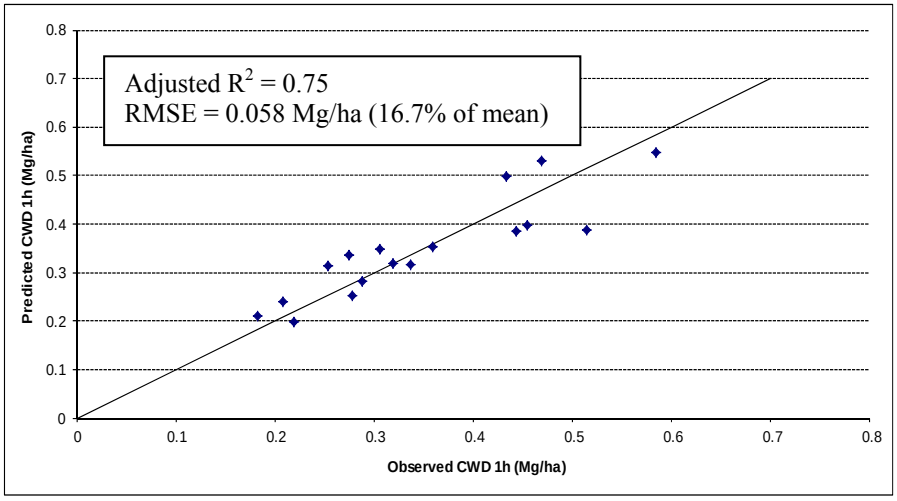

Figure 5: The observed vs. predicted plot for CWD modeling based on Kriging (10m) for 1h fuels.

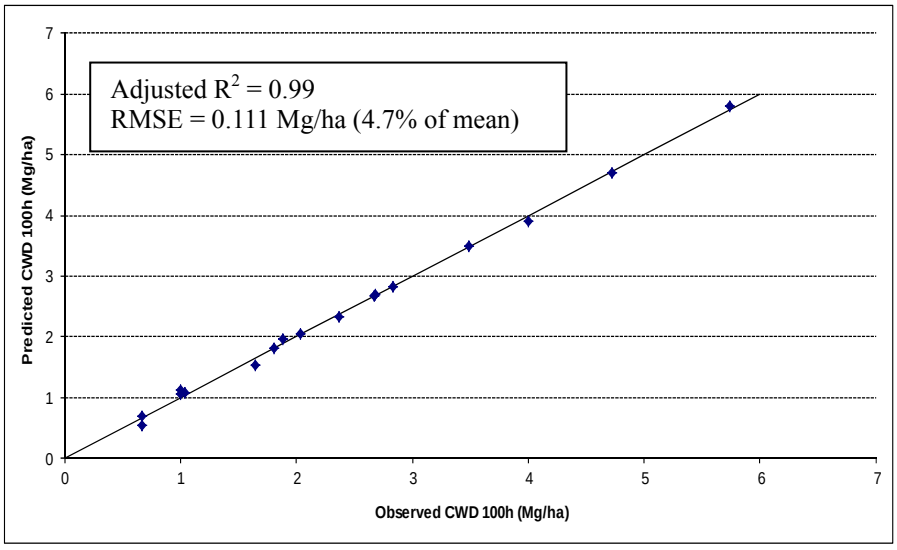

Figure 6: The observed vs. predicted plot for CWD modeling based on Kriging (10m) for 100h fuels.

4. Discussion

The best CWD model fits had high adjusted R^2 values of between 0.77-0.99, although models exhibited a range of adjusted R^2 and RMSE values. The models based on Kriging at 10m spatial resolution performed best, especially in the case of the intermediate CWD fuel loads (10h and 100h). Models with more independent variables performed better, as expected; however, these models also included a more balanced mix of negative residual ("below-ground") and positive (above-ground) distributional variables when compared to models with fewer independent variables. These independent variable sets included specifically percentile, intensity, maximum, and range metrics, similar to findings by Means *et al.* (2000) and van Aardt *et al.* (2006). These two studies focused on above-ground forest volume and biomass estimation and it is interesting to note that the approach could potentially be extended to CWD modeling, as indicated by the results.

The selection of Kriging and a 10m spatial resolution as best performing models was attributed to the smoother, accurate interpolation due to Kriging (van Aardt *et al*., 2006) and the manner in which 10m DEM grid cells partition the LiDAR height distribution; this latter aspect needs to be explored more fully in future studies. The low RMSE values (<10% of the mean) for medium-slow and medium-fast burning fuels were encouraging, while the high RMSE in the case of 1000h CWD fuel weight (47% of the mean) was attributed to the small sample and number of independent variables. Finally, we concluded that, depending on the application, there is evidence that previously considered "erroneous" return values could be useful as indicators of fine-scale structure close to the ground surface. This especially was evidenced by inclusion of negative residual intensity and range values, which show that such delayed signals are useful for modeling structures close to the ground surface. However, this approach requires significant validation across regions, since industry experts (e.g., Joe Liadsky, Optech system engineer, *personal communication*) expressed doubts that multiple scattering could be detected at narrow beam divergence angles (0.56 mrad), even though he acknowledged that there is evidence of "structure" in the signal.

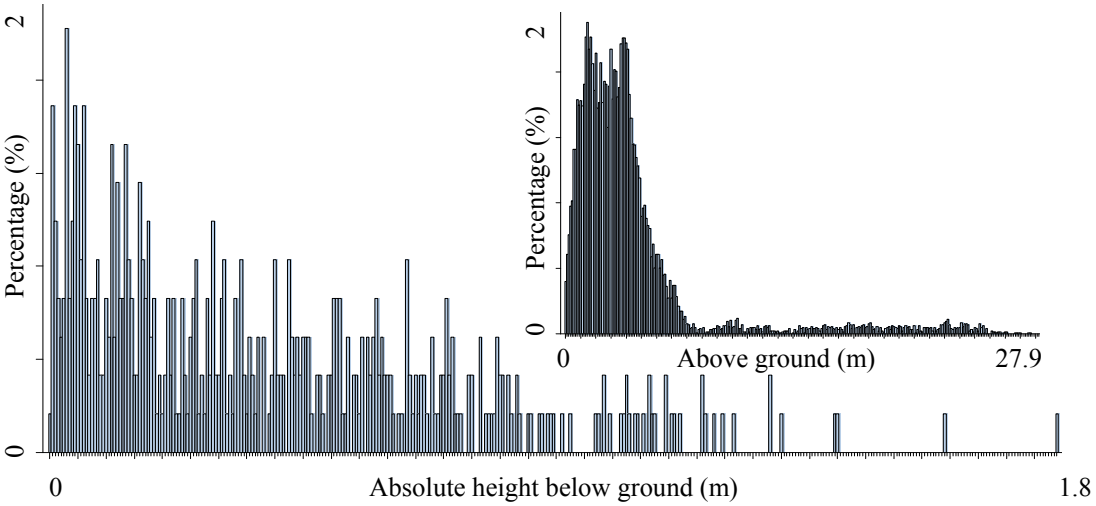

Figure 7: Below-ground and above-ground (inset) LiDAR return distributions for the plot that exhibited the smallest RMSE for CWD modeling based on Kriging (10m) for 100h fuels.

4. Conclusions

We have shown that consideration of close-to-ground multiple scattering in CWD fuel load modeling is justified. This was corroborated by the inclusion of negative LiDAR return DEM residuals as part of the independent variable set in most CWD models. Fusion of above-ground and scattered/delayed returns appeared to work best in the case of medium-fast (10h) and medium-slow (100h) burning fuels. This was attributed to lack of a distinct signal for fine 1h fuels and very coarse 1000h fuels, resulting in limited or dampened LiDAR responses, respectively. Future research will focus on validating the approach by increasing the sample size and the LiDAR point density, and testing across diverse regions.

Acknowledgements

We would like to thank Kucera International for the LiDAR data collection. This work was supported in part by the National Science Foundation's Partnerships for Innovation Program (# 0917839) and the United States Department of Agriculture (USDA; #3049024176-11-419).

References

Blankenship B.A. and M.A. Arthur, 2006. Stand structure over nine years in burned and fire-excluded oak stands on the Cumberland Plateau, Kentucky. *Forest Ecology and Management* 225: 134-145.

Brose P., T. Schuler, D. Van Lear and J. Berst, 2001. Bringing fire back: the changing regimes of the Appalachian mixed-oak forests. *Journal of Forestry* 99: 30-35.

Brown J.K., R.D. Oberheu, and C.M. Johnston, 1982. Handbook for inventorying surface fuels and biomass in the interior West. *General Technical Report INT-129*. Ogden, UT: USDA Forest Service, Intermountain Forest and Range Experiment Station.

Hall S.A., I.C. Burke, D.O. Box, M.R. Kaufmann, and J.M. Stoker, 2005. Estimating stand structure using discrete-return LiDAR: an example from low density, fire prone ponderosa pine forests. *Forest Ecology and Management* 208:189-209

Lefsky M.A., W.B. Cohen, S.A. Acker, G.G. Parker, T.A. Spies, and D. Harding, 1999. LIDAR remote sensing of the canopy structure and biophysical properties of Douglas-fir/western hemlock forests. *Remote Sensing Environment* 70, 339–361.

McEwan, R.W., T.F. Hutchinson, R.P. Long, R.D. Ford, and B.C. McCarthy, 2007. Temporal and spatial patterns of fire occurrence during the establishment of mixed-oak forests in eastern North America. *Journal of Vegetation Science* 18: 655-664.

Means J.E., S.A. Acker, B.J. Fitt, M. Renslow, L. Emerson, and C.J. Hendrix, 2000. Predicting forest stand characteristics with airborne scanning LiDAR. *Photogrammetric Engineering and Remote Sensing* 66(11):1367-1371.

Mutlu M., S.C. Popescu, C. Stripling, and T. Spencer, 2008. Mapping surface fuel models using LiDAR and multispectral data fusion for fire behavior. *Remote Sensing of Environment* 112: 274–285.

Næsset, E., 2002. Predicting forest stand characteristics with airborne scanning laser using a practical two-stage procedure and field data. *Remote Sensing of Environment* 80:88-99.

Nelson, R., W. Krabill, and J. Tonelli, 1988. Estimating forest biomass and volume using airborne laser data. *Remote Sensing of Environment* 24:247-267.

Pesonen, A., M. Maltamo, K. Eerikäinen, and P. Packalén, 2008. Airborne laser scanning based prediction of coarse woody debris volumes in a conservation area. *Forest Ecology and Management* 255: 3288–3296.

Popescu, S.C., R.H. Wynne, and J.A. Scrivani, 2004. Fusion of small-footprint LiDAR and multispectral data to estimate plot-level volume and biomass in deciduous and pine forests in Virginia, U.S.A. *Forest Science* 50(4):551-565.

Riaño D., E. Meier, B. Allgower, E. Chuvieco, and S.L. Ustin, 2003. Modeling airborne laser scanning data for the spatial generation of critical forest parameters in fire behavior modeling. *Remote Sensing of Environment* 86: 177−186.

Seielstad C. A. and L.P. Queen, 2003. Using airborne laser altimetry to determine fuel models for estimating fire behavior. *Journal of Forestry*, *101*, 10-15.

Skowronski N., K Clark, R. Nelson, J. Hom, and M. Patterson, 2007. Remotely sensed measurements of forest structure and fuel loads in the Pinelands of New Jersey. *Remote Sensing of Environment* 108: 123–129.

van Aardt, J.A.N., R.H. Wynne, and R.G. Oderwald, 2006. Forest Volume and Biomass Estimation Using Small-Footprint LiDAR-Distributional Parameters on a Per-Segment Basis. *Forest Science* 52 (6):636-649.

Wu J., J.A.N. van Aardt, G. P. Asner, R. Mathieu, T. Kennedy-Bowdoin, D. Knapp, K. Wessels, B.F.N. Erasmus, and I. Smit, 2009. Connecting the dots between laser waveforms and herbaceous biomass for assessment of land degradation using small-footprint waveform lidar data. *Proceedings of the 2009 IEEE IGARSS*, July 13-17, 2009, South Africa, 4p.

Zheng G. and L.M. Moskal, 2009. Retrieving Leaf Area Index (LAI) Using Remote Sensing: Theories, Methods and Sensors. *Sensors* 9(4):2719-2745.